sciendo International Conference KNOWLEDGE-BASED ORGANIZATION
Vol. XXVIII No 3 2022

ON THE CALCULUS OF FUNCTIONALLY GRADED PLATES

Vasile NĂSTĂSESCU*, Ghiță BÂRSAN, Silvia MARZAVAN***

***"Ferdinand I" Military Technical Academy, Bucharest, Romania**
****"Nicolae Bălcescu" Land Forces Academy, Sibiu, Romania,**
Academy of Romanian Scientists, Bucharest, Romania
nastasescuv@gmail.com

Abstract: *This paper presents some of our results regarding calculus of the functionally graded plates (FGPs). Such plates are made of Functionally Graded Materials (FGMs), which represent a new material class belonging to the composite materials. Our paper presents some material laws in a comparative way. But the main purpose of this paper is to provide calculus concepts and calculus methodologies, based on the means available in scientific research of mechanical engineering field, for the calculation of plates made of FGMs. Thus, the authors use the concepts of multilayer plate and equivalent plate, using both analytical and numerical calculus. The numerical method used are the Finite Element Method (FEM).The calculation aims both to determine the displacements and the stresses of the plates under statical loads, as well as to determine the free vibration frequencies. The research methodology is based on combining analytical calculation, where and when possible, with numerical simulation. The validation of our results is done by comparison with the analytical solution and the comparative analysis of the methods.*

Keywords: Functionally graded materials, Functionally graded plate, Material property law, Multilayer plate

1. Introduction

During the years 1980, appeared in Japan a new material concept, a new material [1], for avoiding the local stress concentration by sudden changes in material properties.

Materials whose elastic, physical, or mechanical properties vary in thickness, according to a law, are called Functionally Graded Materials (FGMs) [2], [3], [5].

Such materials are made of two materials, usually with very different properties [4], [5]. Through special technologies, through proportions established between the two materials based on a material law, the properties vary continuously from the highest values (at the top) to the lowest values (at the bottom) – Figure 1.

FGMs are part of the large category of composite materials, capable of being used in many fields [6].

The structural elements, made of such materials, are plates and beams, often named Functionally Graded Plates (FGPs), respectively Functionally Graded Beams (FGBs).

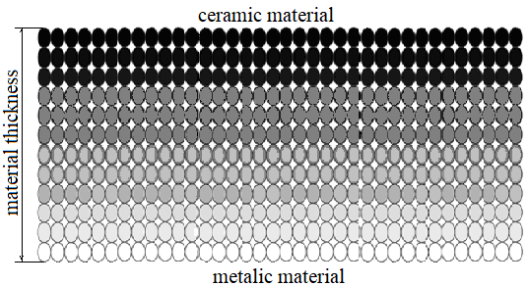


Figure 1: A changing composition model of a FGMs

DOI: 10.2478/kbo-2022-0090
© 2015. This work is licensed under the Creative Commons Attribution-Non Commercial-No Derivatives 3.0 License.

The Functionally Graded Materials concept has developed, and it is still under developing, both in terms of the manufacturing and also in terms of calculus.
The current importance of FGMs is a very high one, due to their special properties, which makes them suitable for use in many fields such as aerospace, chemical plant, electronics, energy conversion, mechanical engineering, nuclear energy, biomaterials and in many other fields. Several material laws are known and used: the Reuss law, the Voigt law, the law of the local representative volume element (LRVE), the Mori-Tanaka law, the exponential law, the power law and others. All these laws are synthetically presented in the next chapter.
The finite element method is used in its general form, well known and used in mechanical engineering. The program used is Ansys/LsDyna; the use of this software (widely accessible and reliable for specialists) allowed us to use, in addition to the usual finite element, a special finite element - the multilayer finite element.

2. Material Properties Laws

The continuous variation of the properties, on the thickness of the plate, takes place according to one of the material laws adopted by the manufacturer.
The geometric model of the definition of material laws is presented in Figure 2. The indices *"t"* and *"b"* in the definition relations refer to the top and bottom respectively faces of the plate [7].

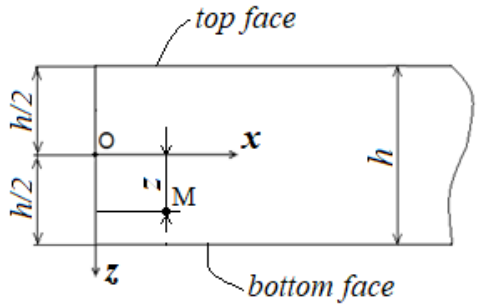


Figure 2: Geometrical model of a FGP

2.1. Reuss Law

Any property, like Young's modulus E, is a function $E(z)$ of coordinate z which is represented by the next relationship (Mishnaevsky 2007), where V_t is the volume fraction of the top material (let's say ceramic) and it is calculated by the relation (2).

$$E(z)=\frac{E_t E_b}{E_t\left(1-V_t\right)+E_b V_t} \tag{1}$$

$$V_t=\left(\frac{1}{2}+\frac{z}{h}\right)^k \tag{2}$$

In the relations (1) and (2) the following notations were used: $E(z)$ is Young modulus in a point with z coordinate; E_t is Young modulus at the level of top surface; h is the thickness of the plate (Figure 2) and k is the power coefficient, which may have different values, less or greater than 1.

2.2. Voigt Law

This model is used in many FGMs analysis. With the same notations, the Voigt law is represented by the relation (3).

$$E(z)=E_t V_t+E_b\left(1-V_t\right) \tag{3}$$

2.3. Local Representative Volume Element (LRVE) Law

This model is based on a mesoscopic length scale, which is much larger than the characteristic length scale of the component particles, but smaller than the characteristic length scale of a macroscopic specimen (Ju and Chen 1994).

$$E(z)=E_b\left(1+\frac{V_t}{FE-\sqrt[3]{V_t}}\right) \tag{4}$$

$$FE=\frac{1}{1-E_b/E_t} \tag{5}$$

The LRVE law is based on the hypothesis according to which the microstructure of the heterogeneous material is known.
The main input parameter is represented by the average volume or the overall average of the microstructure descriptors.

Relations (4) and (5) represent the mathematical expression of the LRVE law (Akbarzadeh *et. al.* 2015).

2.4. Mori-Tanaka Law

In this model, the heterogeneous material of FGM is considered a composite with two materials, one being the material consolidated by spherical particles (the other material) distributed randomly.

$$E(z) = E_b + (E_t - E_b) \times \\ \times \frac{V_t}{1 + (1 - V_t) \cdot (E_t / E_b - 1) \cdot \frac{(1+\nu)}{3(1-\nu)}} \qquad (6)$$

In general, the variation of the Poisson's ratio ν is small and as a result its influence on FGM behavior is small (Kitipornchai 2006). Consequently, in this model and in our research, the Poisson's ratio was considered constant.

2.5. Exponential Law

Relation (7) and (8) represent the exponential law used in the construction of FGMs. The notations used are those described above in this paper.

$$E(z) = E_t \cdot \exp^{\left[-\lambda\left(1-\frac{2z}{h}\right)\right]} \qquad (7)$$

$$\lambda = \frac{1}{2}\ln\left(\frac{E_t}{E_b}\right) \qquad (8)$$

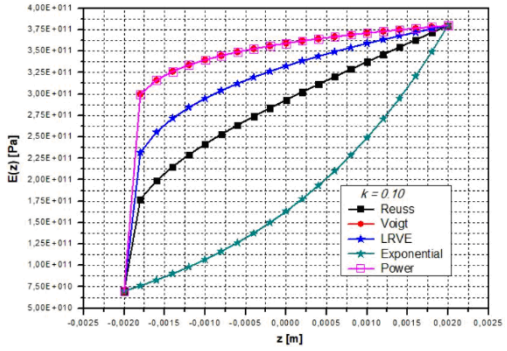
2.6. Power Law

This model is the most used both for the description and obtaining of the properties and in the development of the calculations regarding the deformations and tensions.

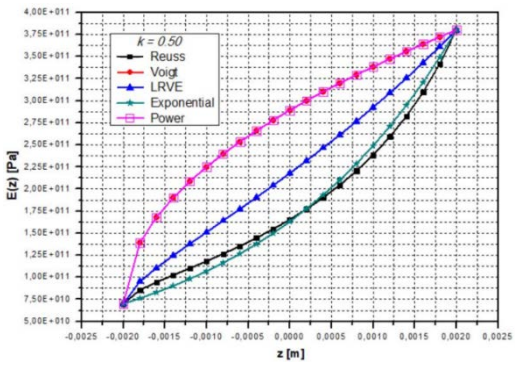
$$E(z) = E_b + (E_t - E_b)\left(\frac{1}{2} + \frac{z}{h}\right)^k \qquad (9)$$

2.7. Graphical representations of the material laws

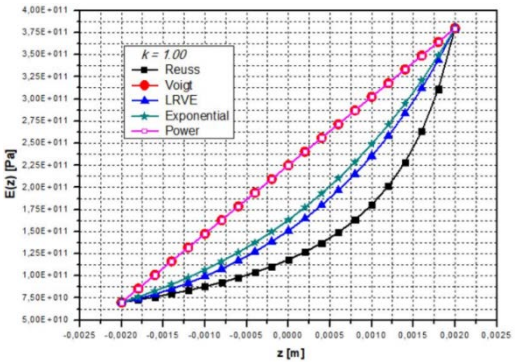
This graphical representation are referring to a functionally graded plate with a thickness of 0.004 m, made of two materials, having: $E_t = 3.8 \cdot 10^{11}$ [Pa] and $E_b = 7 \cdot 10^{10}$ [Pa].



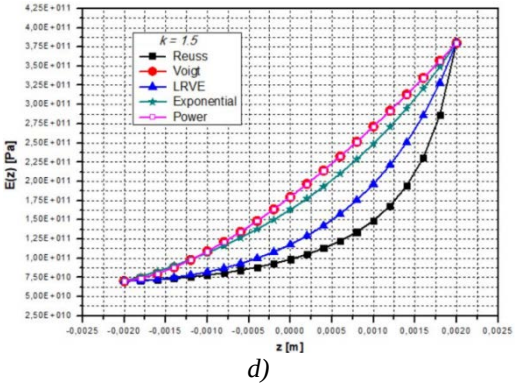
a)



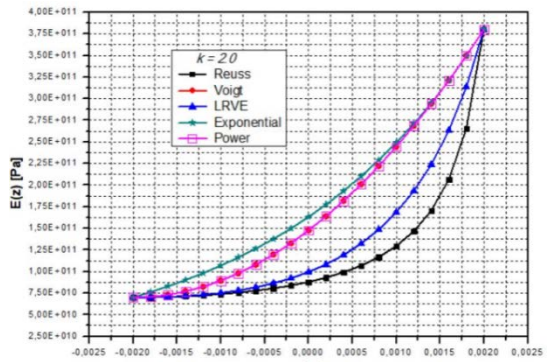
b)



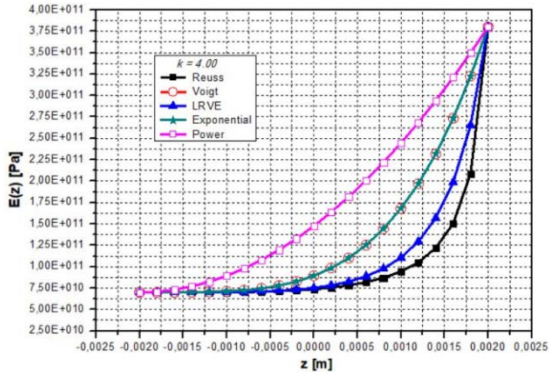
c)



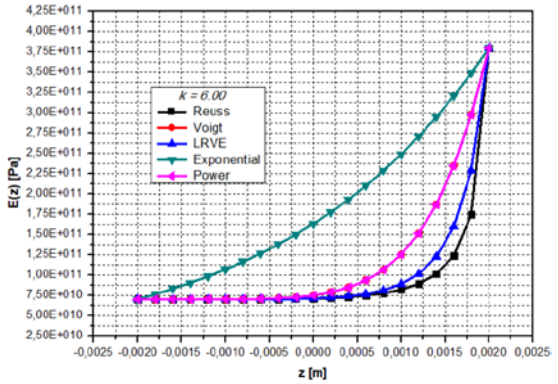
d)



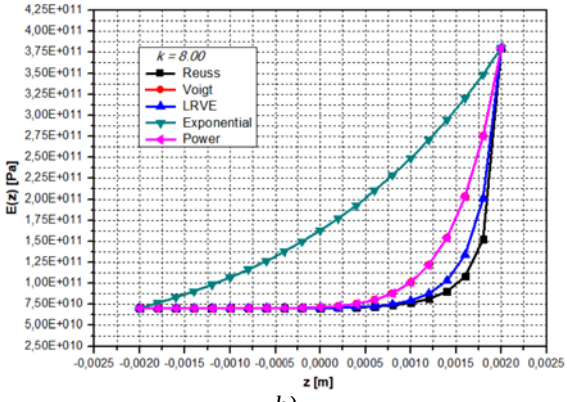
e)



f)



g)



h)

Figure3: Evolution of some functions E (z) for different k values

In the Figures 3*a)...3h)*, the laws of the Young's modulus, used in functionally graded materials are graphically presented, in a comparative way, for different values of the power law coefficient k.

The curve x of other properties (shear modulus G, Poisson ratio ν, density ρ etc.) have the same shape, but the values are different.

One of the most used law of variation of material properties is the power law - the relation (9). In our research, in the numerical simulations performed by us, this law was used.

In the Figure 3, the variation of Young's modulus is presented, versus z coordinate for different values of power law coefficient *k.*

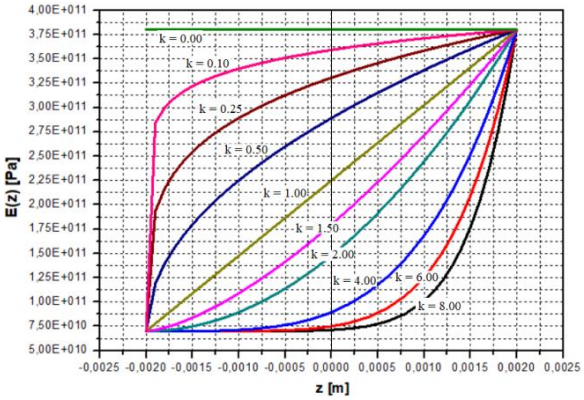


Figure 4: The influence of the power coefficient k upon power law curves

Looking at Figure 4, we can see that for values much smaller than 1 and much larger than 1, the variation of *E(z)* is very strong, in the sense of approaching the values of the top layer, respectively of the bottom layer.

3. Analytical Solution

3.1. Multilayer plate concept

The concept of multilayer plate consists in changing the continuous variation of the elastic properties (Figures 3 and 4) with a step variation (Figure 5).

The concept of multilayer plate involves the composition of FGPs from a number of layers, each layer being homogeneous and

isotropic but with different properties, constant on the thickness of the layer (Figure 6).

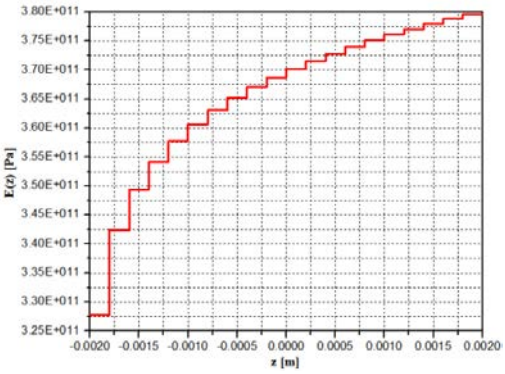


Figure 5: E(z) curve along the thickness by layers

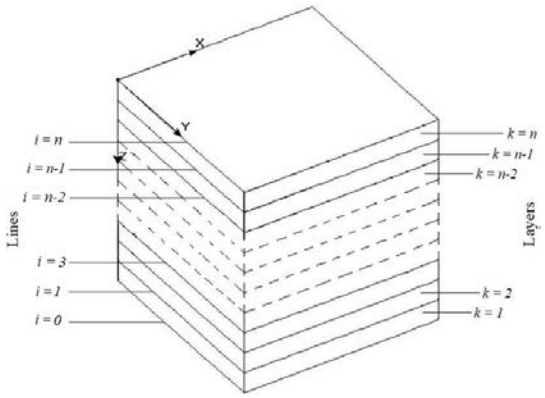


Figure 6: Element of a multilayered plate

For such a plate [10], there is an analytical solution that is obtained by calculating the equivalent or transformed flexural or bending rigidity D^*.
So, the governing differential equation of the laminated plates is [10].

$$\nabla^2\nabla^2 w(x,y) = p_z(x,y)/D^* \tag{10}$$

where:

$$D^* = \frac{A\cdot C - B^2}{A} \tag{11}$$

$$A = \sum_k \frac{E_k}{1-\upsilon_k^2}\cdot\left(z_k - z_{k-1}\right) \tag{12}$$

$$B = \sum_k \frac{E_k}{1-\upsilon_k^2}\frac{z_k^2 - z_{k-1}^2}{2} \tag{13}$$

$$C = \sum_k \frac{E_k}{1-\upsilon_k^2}\cdot\frac{z_k^3 - z_{k-1}^3}{3} \tag{14}$$

The index k, in the relations (12)...(14) refers to the k^{th} layer, as in the Figure 5.
Our experience leads us to the conclusion that the thickness of a layer (th_L) would have to be determined by the relation:

$$th_L \le h/20\ [m] \tag{15}$$

Such a value of th_L allowed us to get acceptable results (less than 3%) compared to the analytical solutions.
For a circular plane plate, the relation (10) becomes:

$$\nabla^2\nabla^2 w(r) = p_z/D^* \tag{16}$$

3.2. Direct integration

Starting from the well-known calculus relation of the bending moment, in which the reference system was used with its origin in a plane that divides the thickness of the plate into two equal parts, we can write:

$$M_x = \int_A z\sigma_x dA =$$

$$= -\left(\frac{\partial^2 w}{\partial x^2} + \nu\frac{\partial^2 w}{\partial y^2}\right)\int_{-\frac{h}{2}}^{\frac{h}{2}} \frac{E(z)z^2}{1-\nu^2}\mathrm{dz} = \tag{17}$$

$$= -D\left(\frac{\partial^2 w}{\partial x^2} + \nu\frac{\partial^2 w}{\partial y^2}\right)$$

From relation (17), it follows that the calculus relation of the bending stiffness of the plate is represented by the relation (13), when the variation of the Poisson's ratio along the thickness is neglected:

$$D = D_a = \frac{1}{1-\nu^2}\int_{-\frac{h}{2}}^{\frac{h}{2}} E(z)\cdot z^2\cdot \mathrm{dz} \tag{18}$$

Using the material power law -relation (9) – by solving the integral contained in relation (18) the following result is obtained:

$$D = D_a = \frac{E_b h^3}{12(1-\nu^2)} + \frac{(E_c - E_b)h^3}{1-\nu^2} \times \times \left[\frac{1}{3+k} - \frac{1}{2+k} + \frac{1}{4(k+1)} \right] \quad (19)$$

The solution of the relation (18) can also be obtained using Mathcad software.

3.3 Equivalent plate concept

The concept of equivalent plate preserves the general (shape and dimension) geometry of the plate, so that the spatial distribution of the masses is preserved, and this fact is very important in the modal analysis and dynamic response of the structure. Preserving the general geometry is also important for defining parameters and/or determining the response at any point in the given structure.

The concept of equivalent plate is a plate with homogeneous and isotropic properties, but these properties are fictitious, virtual, equivalent.

The concept of equivalent plate involves that all other elastic characteristics to have equivalent values, so that the equivalent plate behaves identically to the real plate.

Having regard to the general equation of the transverse displacement of a plate under load– relation (10) -it follows that the equivalent plate must have the same bending rigidity D_{eq} with the real plate:

$$D_{eq} = D_a \quad (20)$$

4. Illustrative Example

4.1. Analytical calculus of displacements

It is considered a circular plane plate, made of FGMs, with clamped edges, under an uniform load, like in the Figure 6, having the radius $a = 0.05\,m$, the thickness $h = 0.004\,m$ and the uniform distributed load $p = 5.0 \cdot 10^6\ Pa$.

The material properties are presented in Table 1.

Table 1 Material properties

Materials:	Metal ceramic Al_2O_3	Metal aluminum
Position:	Top	Bottom
$E\,[Pa]$	$3.8 \cdot 10^{11}$	$7 \cdot 10^{10}$
$\nu\,[-]$	0.30	0.30
$\rho\,[kg/m^3]$	3960	2700

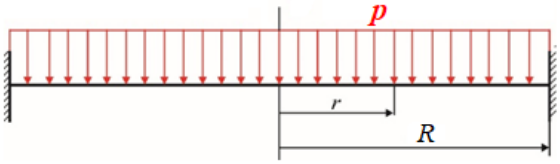


Figure 7: A circular functionally graded plate

Using the multilayer plate concept requires assigning the elastic properties to each layer, according to the curve in Figure 5. Given the relation (15), we considered the plate composed of 20 layers.

Table 2 The values of density for each layer

$z_{layer}^{av.}$ [m]	$E(z_{layer}^{av})$ [Pa]	$\rho\left(z_{layer}^{av.}\right)$ [kg/m^3]
-0.0019	3.27786E+11	3.74777E+03
-0.0017	3.42342E+11	3.80694E+03
-0.0015	3.49388E+11	3.83558E+03
-0.0013	3.54128E+11	3.85484E+03
-0.0011	3.57721E+11	3.86944E+03
-0.0009	3.60622E+11	3.88124E+03
-0.0007	3.63060E+11	3.89115E+03
-0.0005	3.65164E+11	3.89970E+03
-0.0003	3.67019E+11	3.90723E+03
-0.0001	3.68673E+11	3.91396E+03
0.0001	3.70172E+11	3.92005E+03
0.0003	3.71540E+11	3.92561E+03
0.0005	3.72800E+11	3.93073E+03
0.0007	3.73967E+11	3.93548E+03
0.0009	3.75055E+11	3.93990E+03
0.0011	3.76074E+11	3.94404E+03
0.0013	3.77033E+11	3.94794E+03
0.0015	3.77937E+11	3.95162E+03
0.0017	3.78794E+11	3.95510E+03
0.0019	3.79608E+11	3.95841E+03

In Table 2, the values of the properties of each layer (Young's modulus and density) are presented, for the power law – relation (9) - and for the value of the power coefficient $k = 0.05$.

Using the relations (11) ... (14), the respective parameters have the values:

$$A = 1.60635E + 09 \left[Pa \cdot m\right] \quad (21)$$

$$B = 3151337.97 \, [Pa \cdot m^2] \quad (22)$$

$$C = 8298.11 \, [Pa \cdot m^3] \quad (23)$$

$$D^* = 2115.80 \, [Pa \cdot m^3] \quad (24)$$

The bending rigidity of the plate, calculated using relation (15), has the value:

$$D_a = 2114.30 \, [Pa \cdot m^3] \quad (25)$$

Between D^* and D_a, the error is only 0.07%. This finding shows that both methods are valid for the functionally graded material plates calculation. In practice, any value of D^* or D_a can be the *equivalent stiffness* of the functionally graded plate D.

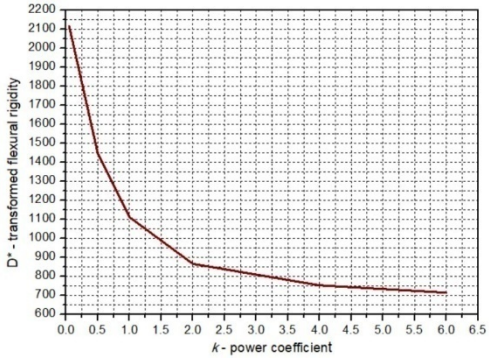


Figure 8: Flexural rigidity versus power coefficient k

By repeating the calculations for other values of the power coefficient k, the data necessary for the graphical representation in Figure 8 are obtained. The curve $D(k)$ in Figure 8 shows that as the values of k increase, the bending stiffness of the plate decreases.

The calculus of the maximum transverse displacement (it occurs in the center of the plate) is calculated with the relation [10],

$$w_{\max} = \frac{pa^4}{64D} \quad (25)$$

which leads to the following result:

$$\begin{cases} w^a_{\max} = \dfrac{pa^4}{64D_a} = 0.000230942\,[m] \\ w^*_{\max} = \dfrac{pa^4}{64D^*} = 0.000230778\,[m] \end{cases} \quad (26)$$

The error between the values of $w^m_{\max}$ and $w^a_{\max}$ is only 0.07 percent. Practically, we can consider only one value of the analytical calculus, namely:

$$w_{\max} = 0.000231\,[m] \quad (27)$$

In the above analytical calculus, the multilayer plate concept was used to determine the stiffness, and the displacement calculation was performed based on the equivalent plate concept.

4.2. FEM calculus of the displacements

The numerical calculation by the finite element method was performed in three variants: I - equivalent plate model with ordinary finite elements, II - multilayer plate model with ordinary finite elements and III - multilayer plate model with multilayer finite elements.

One of the most important parameters in the analysis with FEM is Young's module. It was extracted from the previously calculated plate stiffness:

$$E^* = \frac{12(1-\nu^2)\cdot D^*}{h^3} = \quad (28)$$
$$= 3.610084 \cdot 10^{11} \, [Pa]$$

In the analysis with FEM we used a 3D model, with 3 dimensions of the finite elements: 1, 2 and 3 mm; the calculation model was a quarter of the structure, the plate having two axes of symmetry.

Table 3 Analytical and numerical results

ANALYTICAL RESULT						
w_{max} **[m]**			**0.000231**			
FE size	**FINITE ELEMENT RESULTS**					
	Equivalent plate (E^*, homogeneous and isotropic plate) **Model I**		**Multilayered plate** (Each layer is isotropic and homogeneous, **common FE**) **Model II**		**Multilayered plate** (Each layer is isotropic and homogeneous, **multilayered FE**) **Model III**	
	w_{max} **[m]**	***Er. [%]***	w_{max} **[m]**	***Er. [%]***	w_{max} **[m]**	***Er. [%]***
1.0 mm	0.000231	***0.00***	0.000234	***1.30***	0.000236	***2.16***
2.0 mm	0.000225	***-2.60***	0.000228	***-1.30***	0.000236	***2.16***
3.0 mm	0.000218	***-5.63***	0.000220	***-4.76***	0.000236	***2.16***

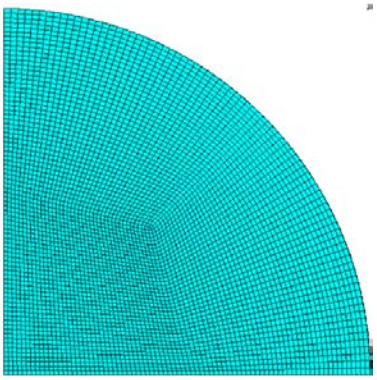


Figure 9: The 3D finite element model

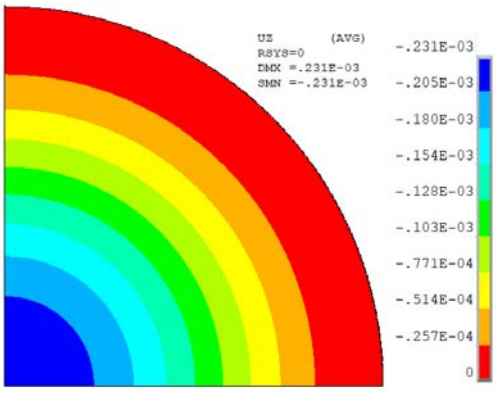


Figure 10: Displacement field for Model I

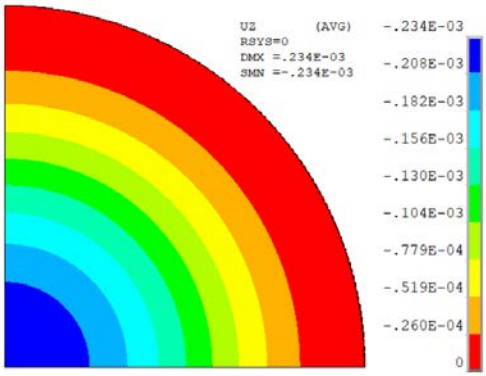


Figure 11: Displacement field for Model II

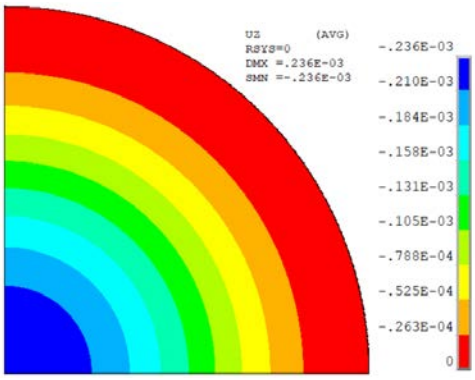


Figure 12: Displacement field for Model III

The finite element Solid185 (brick with eight nodes), from Ansys finite element library was used. This finite element can be also used with the multilayer option. The 3D finite element model is presented in the Figure 9, the FE size being 0.001 m.
The results of the displacement calculus are comparatively presented in Table 3. These results and the errors show us the validity of the concepts, methods and methodologies used for problem solving.

4.3. Analytical calculus of stresses

Using the known relationships from plate theory [10], in clamped section, radial and tangential stresses are calculated with de relations:

$$\sigma_r = -z\frac{E}{1-\upsilon^2}\cdot\frac{pR^2}{8D} \tag{29}$$

$$\sigma_\theta = -z\cdot\nu\frac{E}{1-\upsilon^2}\cdot\frac{pR^2}{8D} \tag{30}$$

The maximum values of the stresses occur at the level of the extreme faces ($z=\pm h/2$) and have the values:

$$\sigma_r = -z\frac{E_a}{1-\upsilon_{layer}^{2\ 2}}\cdot\frac{pR^2}{8D_a} = 585.893\ [\text{MPa}] \tag{31}$$

$$\sigma_t = \nu\cdot\sigma_r = 129.30\ [\text{MPa}] \tag{32}$$

In the center of the plate, the maximum values of the stresses also occur at the level of the extreme faces ($z=\pm h/2$) and have the values:

$$\sigma_r = \sigma_t = z\frac{E}{1-\upsilon^2}\cdot\frac{pR^2}{16D} \tag{33}$$

$$\sigma_r = \sigma_t = z\frac{E_a}{1-\upsilon_{layer}^2}\cdot\frac{pR^2}{16D_a} = 351.750\ [\text{MPa}] \tag{34}$$

4.4. FEM calculus of the stresses

A 2D and 3D FE models were used.
The same three finite element models (I, II, III) were used also for the stress calculus. The 3D FE models are the same for displacements calculus (Figure 9).
The 2D axisimmetric finite element model is presented in the Figure 13, with a finite element size of 1 mm.
The Figures 14, 15 and 16 present the stress field on the deformed state of the plate, for those three cases (I, II, III) which were used in our research.

Table 4 The results of the stress calculus

Maximum stress values		σ_r [MPa]	
		Clamped edges	Plate center
Analytical		**585.893**	**351.750**
F. E. M.	Equivalent plate **(I)**	583.000	344.750
	Err. [%]	***-0.49***	***-1.99***
	Multilayered plate, common FE **(II)**	599.000	333.140
	Err. [%]	***2.24***	***-5.29***
	Multilayered plate, with multilayered FE **(III)**	594.000	351.940
	Err. [%]	***1.38***	***0.05***

The results of the stress studyare presented synthetically in the Table 4.
The comparative analysis of these results demonstrates, with the power of quantitative determinations, the validity of the concepts used.
The calculation of the errors of the results by FEM in relation to the analytical solution, shows us that any of the three models are valid. However, the use of the equivalent plate concept (model I) or model III leads to the best results, the errors being below 2% and even below 1%.

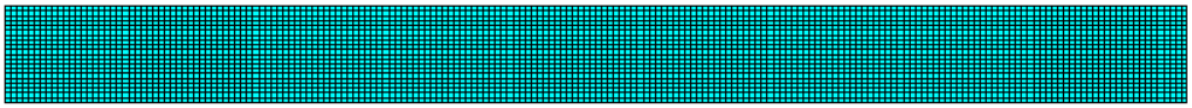


Figure 13: The 2D axisimmetric finite element model

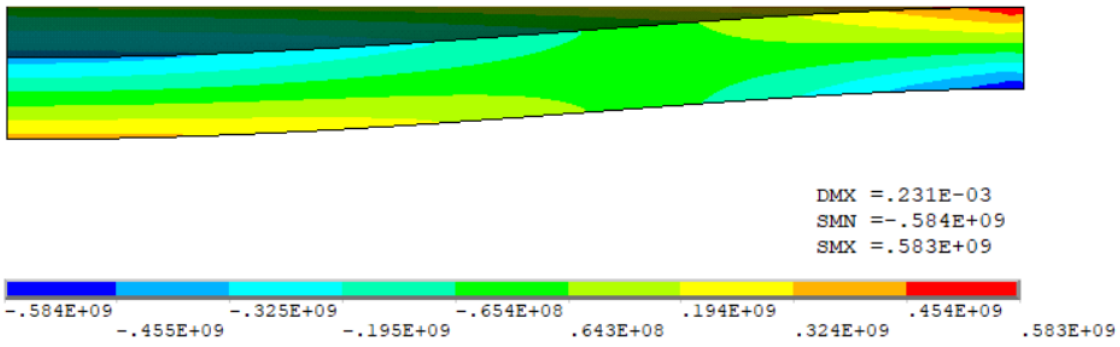


Figure 14: Stress field σ_x, equivalent plate, common FE

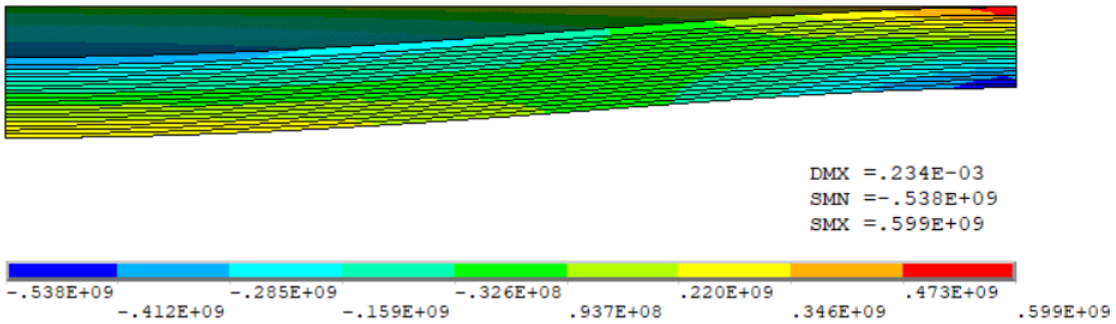


Figure: Stress field σ_x, multilayered plate, common FE

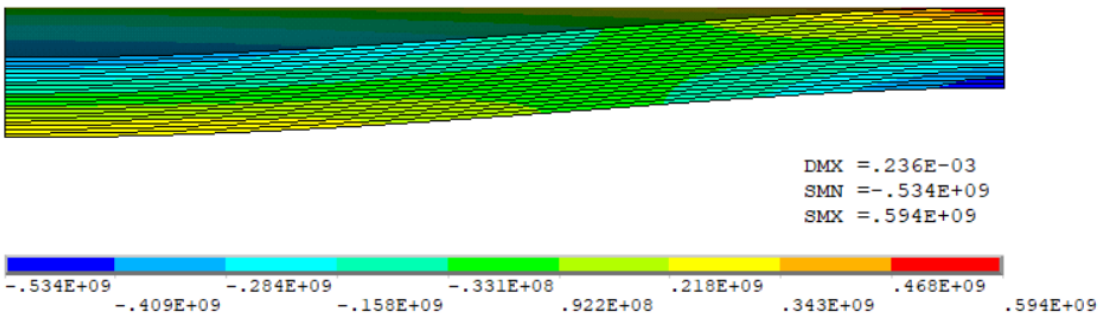


Figure 16: Stress field σ_x, multilayered plate, multilayered FE

The results presented in Table 4 are those obtained using 3D models, in those three cases (I, II, III) – Figures 14…16.

The 2D model (Figure 13) is the simplest model and leads to almost identical results regarding displacements and stresses, but it is not suitable for analyzes such as modal analysis, etc.

4.5. Analytical calculus of free vibrations

For a homogeneous and isotropic plate, we can analytically determine natural frequencies of a thin circular plates, by the relation [11], [15]:

$$f_i = \frac{\alpha_i}{2\pi a^2}\sqrt{\frac{D}{\rho \cdot h}} \qquad (35)$$

where f_i is the natural frequency „i" [Hz], a is the radius [m] of the circular plate, h is the plate thickness [m] and α_i is a constant which depends on the number of nodal circles (s) and the number of nodal diameters (n), according to the data provided by the literature [11], [15].
Some values of these parameters [11] are presented in Table 5; D is the bending rigidity [Pa*m^3] and ρ is the material density [kg/m^3].

Table 5 Values of α_i for n and s parameters

s	$n=0$	$n=1$	$n=2$
0	10.21	21.22	34.84
1	39.78	.....	.....
2	88.90	.....	.....

Nodal circles (s) are those circles, having their centers just in the plate center, at which the displacements are zero during vibration.

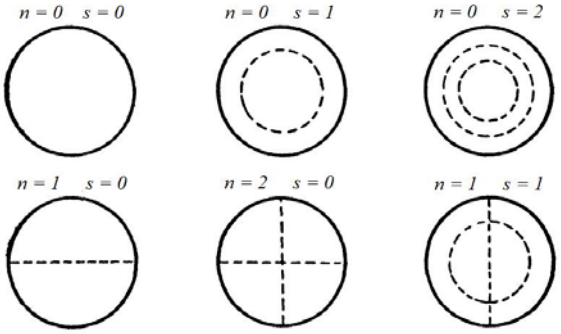


Figure 17: Nodal cricles and nodal diameters

Nodal diameters (n) are those lines (diameters of the circle), along which the deflections during vibration are zero. In the Figure 17 nodale circles and nodal diameters are presented. Using the data from Table 2 and the multilayer plate concept, the eigenfrequencies presented in Table 6 were determined.

Table 6 Some results of natural frequencies by analitical calculus

k = 0.05				
Freq. No.	**D***	**E***	**ρ***	**f**
	Nm	Pa	kg/m^3	Hz
1	2115.8	3.610E+11	3899.94	7571.83
2	2115.8	3.610E+11	3899.94	15732.73
3	2115.8	3.610E+11	3899.94	25830.74
k = 0.50				
Freq. No.	**D***	**E***	**ρ***	**f**
	Nm	Pa	kg/m^3	Hz
1	1449.26	2.473E+11	3539.99	6577.56
2	1449.26	2.473E+11	3539.99	13666.84
3	1449.26	2.473E+11	3539.99	22438.86
k = 1.00				
Freq. No.	**D***	**E***	**ρ***	**f**
	Nm	Pa	kg/m^3	Hz
1	1111.12	1.896E+11	3330.00	5938.15
2	1111.12	1.896E+11	3330.00	12338.27
3	1111.12	1.896E+11	3330.00	20257.55

The frequency values presented in Table 3 show that the frequencies decrease with increasing values of the power coefficient k. This observation is confirmed by the curves shown in Figure 18, based on the data in the Table 3.

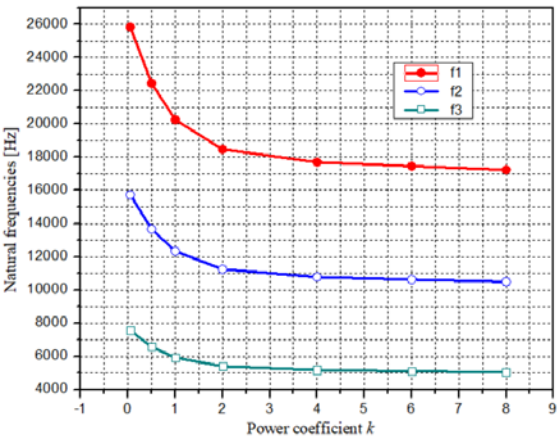


Figure 18: Natural frequencies versus k

The rate of decrease in frequency with the coefficient k is the smallest for the first frequency (Figure 18), and then the rate of

decrease grows up with the number of frequency.
Using the equivalent plate concept requires determining the global values of density and Young's modulus, as follows:

$$E_{ech} = \frac{12(1-\nu^2)}{h^3} D \tag{35}$$

The relation (35) is valid for the assumption of a constant value of the Poisson's ratio.
For the considered problem, taking into account the values calculated above, equivalent Young' modulus (E_{ech}) has the value of 3.61009E+11 Pa. The mass of a plate element is written:

$$dM_{placa} = \rho(z) \cdot dV = \rho(z) \cdot A \cdot dz = \\ = \pi r^2 \cdot \rho(z) \cdot \mathrm{dz} \tag{36}$$

$$M_{placa} = \pi r^2 \int_{-h/2}^{h/2} \rho(z)\mathrm{dz} = A \cdot I_0 \tag{37}$$

$$I_0 = \int_{-h/2}^{h/2} \left[\rho_b + (\rho_t - \rho_b) \cdot \left(0.5 + \frac{z}{h} \right)^k \right] \mathrm{dz} \tag{38}$$

Analytical solution of the integral (38) is:

$$I_0 = \rho_b h + \frac{h}{k+1} (\rho_t - \rho_b) \tag{39}$$

$$M_{placa} = \pi r^2 \cdot I_0 = \pi \cdot 0.05^2 \cdot 15.60 = \\ = 0.12252 \ kg \tag{40}$$

$$V_{placa} = \pi \cdot r^2 \cdot h = \pi \cdot 0.05^2 \cdot 0.004 = \\ = 0.0000314159 \ m^3 \tag{41}$$

As the equivalent density (ρ_{ech}) is concerned, this can be calculated starting from the plate mass.

$$\rho_{ech} = \frac{M_{placa}}{V_{placa}} = 3899.936 \frac{kg}{m^3} \tag{42}$$

Following the curve presented in Figure 19, we notice that both the plate mass and the density vary with the power coefficient k, in the sense of decreasing the mass when the power coefficient increases. The results obtained using the equivalent plate concept are presented comparatively, in Table 7.

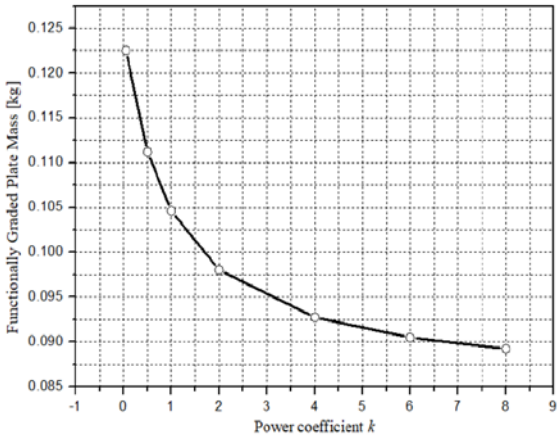


Figure 19: FGMP mass versus power coefficient k

4.6. FE calculus of free vibrations

The equation of free vibrations of a structure, not damped, in the finite element method [9], [10], [11], is,

$$[M]\{\ddot{w}\} + [K]\{w\} = 0 \tag{43}$$

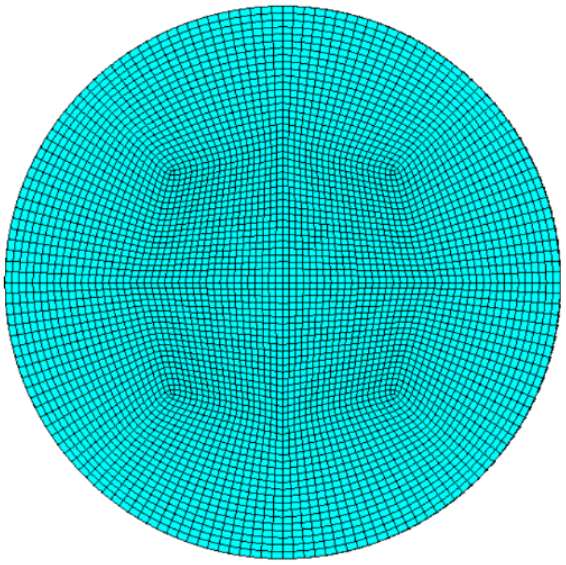
in which $[M]$ is the consistent matrix of the masses of the structure, and $[K]$ is the global matrix of rigidity of the structure. Accepting [12], [13], [14] that the dynamic response of the structure is governed by a harmonic law, the equation (43) becomes:

$$\left([K] - \omega^2 [M] \right) \{\bar{w}\} = 0 \tag{44}$$

The characteristic equation of eigenvalues is of the form:

$$[K]\{\bar{w}_i\} = \lambda_i [M]\{\bar{w}_i\} \tag{45}$$

where $\omega_i^2 = \lambda_i$ are the roots of the characteristic equation and represent the squares of the eigen pulsations of free vibrations expressed in rad/s, called eigenvalues, and $\{\bar{w}_i\}$ are eigen vectors associated with each eigenvalue.

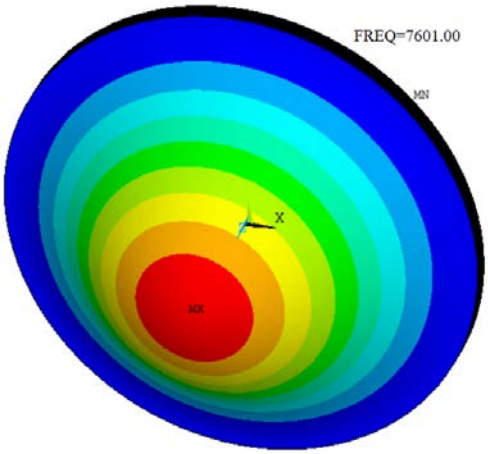


For the calculations with finite elements, three calculus models were used as follows: the equivalent plate model (homogeneous and isotropic), of the plate made of FGMs with the use of the usual Solid185 finite element - **case (I)**, then the real multilayer plate model (20 layers) with the use of the usual Solid185 finite element - **case (II)** and the real multilayer plate model (20 layers), where Solid185 finite element with the multilayer option was used - **case (III)**. For the modal analysis, the finite element model (Figure 20) was for the whole structure, in order to obtain all its own modes of vibration.

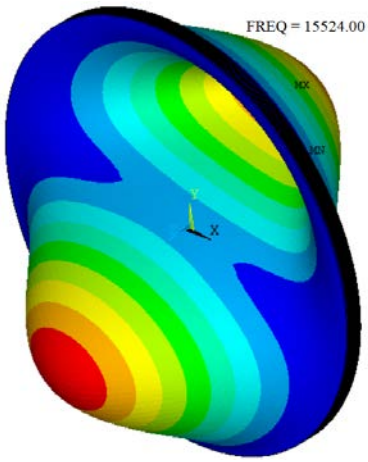
Figure 20: Finite element model

Table 7 Some results regarding natural frequencies [Hz], by FEM calculated

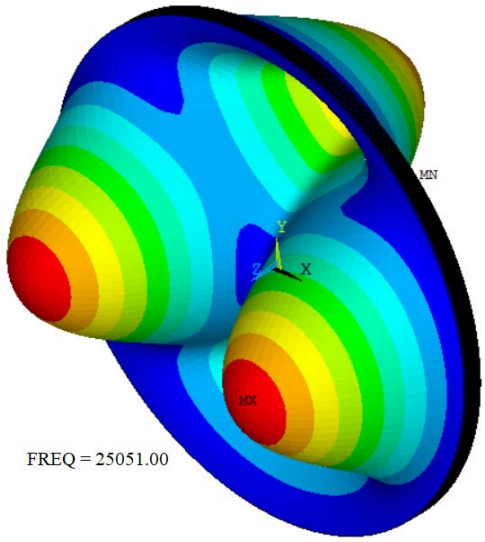
k	Freq. No.	Analytical solution	Equivalent plate *(E*, ρ*)* **(I)**	***Er. [%]***	Multilayer plate *(E, ρ*)* **(II)**	***Er. [%]***	Multilayer plate *(E, ρ*)* **(III)**	***Er. [%]***
0.05	1	7571.83	7582.80	*0.14*	7601.00	*0.39*	7468.70	*-1.36*
	2	15732.73	15479.00	*-1.61*	15524.00	*-1.33*	15335.00	*-2.53*
	3	25830.74	24893.00	*-3.63*	25051.00	*-3.02*	24781.00	*-4.06*
0.50	1	6577.56	6590.20	*0.19*	6587.40	*0.15*	6491.30	*-1.31*
	2	13666.84	13459.00	*-1.52*	13503.00	*-1.20*	13332.00	*-2.45*
	3	22438.86	21714.00	*-3.23*	21813.00	*-2.79*	21549.00	*-3.97*
1.00	1	5938.15	5949.60	*0.19*	6105.50	*2.82*	5858.50	*-1.34*
	2	12338.27	12151.00	*-1.52*	12456.00	*0.95*	12024.00	*-2.55*
	3	20257.55	19603.00	*-3.23*	20154.00	*-0.51*	19422.00	*-4.12*



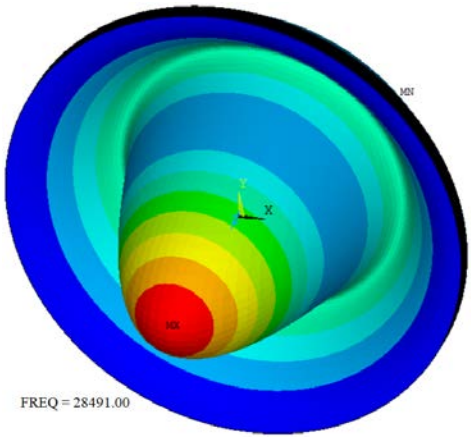
a) First frequency: n = 0; s = 0



b) Second frequency: n = 1 ; s = 0



c) Third frequency: n = 2 ; s = 0



d) Fourth frequency: n = 0 ; s = 1

Figure 21: The shape of first four frequencies of the FGMs plate

Figure 21 shows the proper forms for the first four natural vibrations, obtained by using case (II). The best calculation option remains case (II), which confirms the use of the concept of multilayer plate proposed by the authors.

For this case, the errors are not greater than 5% regardless of the values considered for k .

The first eigen frequencies there is in a very good concordance of the numerical results in relation to the analytical ones. Numerical simulations, including those presented here, show that the errors usually increase with the number of eigen frequencies considered.

5. Conclusions

This paper presents some our researching results regarding numerical calculus of functionally graded plates by using finite element calculus with available professional software.

Our proposed methodology can easily also used for the functionally graded beams.

The authors present an original concept for numerical approaching of functionally graded plates calculus by FEM. This concept is based on multilayered plate, and it is a simple one, efficient, easy to use and accessible to many specialists.

Knowing and analyzing of the material laws together with efficient numerical methods, open the way, to design such materials with desired qualities.

Sometimes the high material properties would have to be predominant on the thickness and sometimes vice versa.

Our research shows us that even with common finite elements, with simple models, it is possible to obtain the best results, like those presented in the Table 7.

Of course, it is possible to consider an increased number of layers for describing the functionally graded plate. Our research was focused upon the most accessible parameters for a finite element analysis.

References List

[1] Hadj Mostefa A., Merdaci S. An Overview of Functionally Graded Materials <<FGM>>, slimanem2016@gmail.com.

[2] Rasheedat M. Mahamood, Esther T. Akinlabi. Functionally Graded Material: An Overview, Proceedings of tthe World Congress on Engineering 2012, Vol. III, WCE 2012, July 4-6, 2012, London, U.K.

[3] Toudehdehghan A., Lim J. W., Foo K. E. and others. A Brief Review of Functionally Graded Materials, MATEC Web of Conferences 131, 03010 (2017), UTP-UMP SES 2017.
[4] Tarlochan F. Functionally Graded Material: A New Breed of Engineered Material, Journal of Applied Mechanical Engineering. 02 (2013). doi:10.4172/2168-9873.1000e115.
[5] Năstăsescu V., Marzavan S. On Functionally Graded Beam Concept, International Conferences, Celebrating Technical Higher Education into "Vasile Alecsandri" University of Bacău, June, 27-29 2018.
[6] Islam M. El-Galy, Bassiouny I. Saleh, Mahmoud H. Ahmed, Functionally graded materials classifications and development trends from industrial point of view, SN Applied Sciences ISSN 2523-3963, Volume 1, Number 11, SN Appl. Sci. (2019) 1:1-23, DOI 10.1007/s42452-019-1413-4.
[7] Ravikiran Kadoli, Kashif, N. Ganesan. Static Analysis of Functionally Graded Beams Using Higher Order shear Deformation Theory, ScienceDirect, Applied Mathematical Modelling 32 (2008) 2509-2525, ELSEVIER, www.sciencedirect.com.
[8] Nakagi M., Wu Y., Shibata Y., Hagihara S. Constitutive modeling of functionally graded material and its application to fracture in FGM, Transactions on Engineering Sciences vol 13, © 1996 WIT Press, www.witpress.com.
[9] Hadji L., Bernard F. Bending and free vibration analysis of functionally graded beams on elastic foundations with analytical validation, Advances in Materials Research, Vol. 9, No. 1 (2020) 63-98.
[10] Szilard R. Theories and Applications of Plate Analysis. Classical, Numerical and Engineering Methods, John Wiley & Sons, Inc., 2004.
[11] Timoshenko S. Vibration Problems in Engineering, Second Edition, D. Van Nostrand Company, Inc., New York, 1937.
[12] Amal E. Alshorbagy, Eltaher M.A., Mahmoud F.F. Free vibration characteristics of a functionally graded beam by finite element method, Applied Mathematical Modelling, Elsevier, 2011.
[13] Ramu I., Mohanty S. C. Modal analysis of Functionally Graded material Plates using Finite Element Method, ScienceDirect, Procedia Materials Science, Elsevier, 2014.
[14] Hadji L., Bernard F. Bending and Free Vibration Analysis of Functionally Graded Beams on Elastic Foundations with Analytical Validation, Advanced in Materials Research, Vol. 9, No. 1 (2020) 63-98.
[15] Leissa W.A. Vibration of Plates, National Aeronautics and Space Administration, Washington, 1969.